Identification and characterization of an endogenous chemotactic ligand specific for FPRL2

Isabelle Migeotte,[1] Elena Riboldi,[3] Jean-Denis Franssen,[4] Françoise Grégoire,[2] Cécile Loison,[4] Valérie Wittamer,[1] Michel Detheux,[4] Patrick Robberecht,[2] Sabine Costagliola,[1] Gilbert Vassart,[1] Silvano Sozzani,[3,5] Marc Parmentier,[1] and David Communi[1]

[1]Institut de Recherche en Biologie Humaine et Moléculaire and [2]Laboratoire de Chimie Biologique et de la Nutrition, Université Libre de Bruxelles Campus Erasme, B-1070 Brussels, Belgium
[3]Section of General Pathology and Immunology, University of Brescia, 25121 Brescia, Italy
[4]Euroscreen s.a., B-6041 Gosselies, Belgium
[5]Istituto di Ricerche Farmacologiche Mario Negri, 20157 Milano, Italy

Chemotaxis of dendritic cells (DCs) and monocytes is a key step in the initiation of an adequate immune response. Formyl peptide receptor (FPR) and FPR-like receptor (FPRL)1, two G protein–coupled receptors belonging to the FPR family, play an essential role in host defense mechanisms against bacterial infection and in the regulation of inflammatory reactions. FPRL2, the third member of this structural family of chemoattractant receptors, is characterized by its specific expression on monocytes and DCs. Here, we present the isolation from a spleen extract and the functional characterization of F2L, a novel chemoattractant peptide acting specifically through FPRL2. F2L is an acetylated amino-terminal peptide derived from the cleavage of the human heme-binding protein, an intracellular tetrapyrolle-binding protein. The peptide binds and activates FPRL2 in the low nanomolar range, which triggers intracellular calcium release, inhibition of cAMP accumulation, and phosphorylation of extracellular signal–regulated kinase 1/2 mitogen-activated protein kinases through the G_i class of heterotrimeric G proteins. When tested on monocytes and monocyte-derived DCs, F2L promotes calcium mobilization and chemotaxis. Therefore, F2L appears as a new natural chemoattractant peptide for DCs and monocytes, and the first potent and specific agonist of FPRL2.

CORRESPONDENCE
Marc Parmentier:
mparment@ulb.ac.be

Abbreviations used: ERK, extracellular signal–regulated kinase; FPR, formyl peptide receptor; FPRL, FPR-like receptor; GPCR, G protein–coupled receptor; HBP, heme-binding protein; MAP, mitogen-activated protein; SEC, size-exclusion column.

DCs and monocytes are critical players in host immune mechanisms. They are able to sense danger signals of diverse origins (various pathogen classes and tissular disturbances such as necrosis and tumor development; reference 1). They are attracted during early phases of inflammatory reactions by a diverse set of chemoattractant molecules, including chemokines, the complement factor C5a, the bacterial peptide FMLP, the lipid metabolite PAF, and the recently identified chemerin (1, 2). Locally, these cells participate to innate immunity through the phagocytosis of microbes or diseased cells and the secretion of a range of bioactive mediators, including cytokines and chemokines. Immature DCs take up and process available antigens and then, under appropriate stimuli, undergo maturation, switch their expression of chemokine receptors from inflammatory to lymphoid homing receptors, and migrate to the draining lymph nodes where they interact with T cells to initiate an appropriate immune response. These various populations of antigen-presenting cells are extremely heterogeneous in terms of morphology and function. These functional differences are partly related to the set of chemoattractant seven-transmembrane, G protein–coupled receptors (GPCRs) they express.

In the 1970's, synthetic FMLP was one of the first identified potent leukocyte chemoattractants. Natural FMLP was later purified from Gram-negative bacteria (3, 4). Its human receptor, formyl peptide receptor (FPR), was cloned in 1990 from a differentiated HL-60 myeloid leukemia cell cDNA library (5). Two human genes encoding the structurally related receptors FPR-like receptor (FPRL)1

The Journal of Experimental Medicine

and FPRL2 were subsequently cloned by low stringency hybridization using FPR cDNA as a probe, and shown to cluster with FPR on human chromosome 19q13.3 (6, 7). In contrast, the murine FPR gene family comprises at least eight distinct genes (Fpr1 and Fpr-rs 1–7), of which six are clustered on chromosome 17, in a region of conserved synteny with human chromosome 19 (8, 9). Fpr1 is considered the murine orthologue of FPR, whereas Fpr-rs1 and Fpr-rs2 share structural and functional similarity with FPRL1. No obvious orthologue of FPRL2 can be determined from a structural viewpoint. Therefore, it appears that the FPR gene cluster has undergone recent and independent gene duplications in various mammalian species, which may also imply functional divergence of the resulting receptor subtypes.

FPR is a high affinity receptor for formyl peptides. Synthetic W hexapeptides were described as efficient surrogate agonists of FPR, whereas the receptor was also reported to respond to HIV-derived peptides, amino-terminal peptides of annexin I, and cathepsin G, although with relatively low potencies (10–12). FPRL1 shares 69% amino acid identity with FPR and displays low affinity for FMLP. However, FPRL1 appears as a remarkably promiscuous receptor, as it is activated by numerous and chemically unrelated ligands. These include the following: the synthetic peptides MMK1 and W hexapeptides; pathogen-derived peptides such as the Hp 2–20 peptide from *Helicobacter pylori* and peptides derived from HIV gp41 and gp120; the lipid lipoxin A4; as well as a variety of host proteins and peptides such as cathelicidin LL37, annexin I and the Ac1-25 and Ac1-11 peptides derived from this protein, the 88–274 fragment of the urokinase receptor, the serum amyloid A protein, the amyloid β peptide Aβ42, the prion protein fragment P106-126, a fragment from the mitochondrial NADH dehydrogenase subunit I, a truncated form of the chemokine CKβ8-1, and the neuroprotective peptide humanin (3, 4, 13, 14). However, the affinity of FPRL1 for these various ligands is often low, and the functional relevance of these interactions is therefore questionable. FPRL2 shares 56 and 83% amino acid identity with FPR and FPRL1, respectively. FPRL2 does not respond to formyl peptides, but it was described as a low affinity receptor for several FPRL1 agonists, namely the annexin I amino-terminal peptide Ac1-25 (15) and the *H. pylori*–derived peptide Hp 2–20 (16, 17). The synthetic hexapeptides WKYMVM and WKYMVm were also described to act partly through FPRL2 on leukocyte populations expressing various combinations of the FPRs and on recombinant cells expressing FPRL2 (18, 19). Therefore, no high affinity endogenous ligand has so far been identified for FPRL2, which can be considered essentially an orphan receptor.

Interestingly, the three FPRs display a quite different expression profile on phagocytic leukocytes. Neutrophils express functional FPR and FPRL1. Monocytes express the three receptors at their surface, whereas monocyte-derived DCs express FPR and FPRL2 when immature and only retain FPRL2 after maturation (19, 20). Thus, the three receptors might play key roles in the differential migration pattern of these antigen-presenting cells. According to the conserved expression of FPRL2 in monocytes and immature and mature DCs, its cognate ligand could be generated all along the trafficking route of these cells from the sites of inflammation and antigen uptake to the secondary lymphoid organs. Thus, we searched for potential agonist(s) in various sources by reverse pharmacology. We identified in the spleen a biological activity specific for FPRL2-expressing cells and characterized it as the first natural ligand displaying both a high affinity and a high specificity for FPRL2. This new acetylated peptide, called F2L (FPRL2 ligand), is a potent chemoattractant for DCs and monocytes.

RESULTS

Isolation and identification of the F2L peptide as an endogenous ligand of FPRL2

As a screening assay, we developed CHO-K1 cell lines co-expressing human FPRL2, apoaequorin, and $G_{\alpha 16}$. This al-

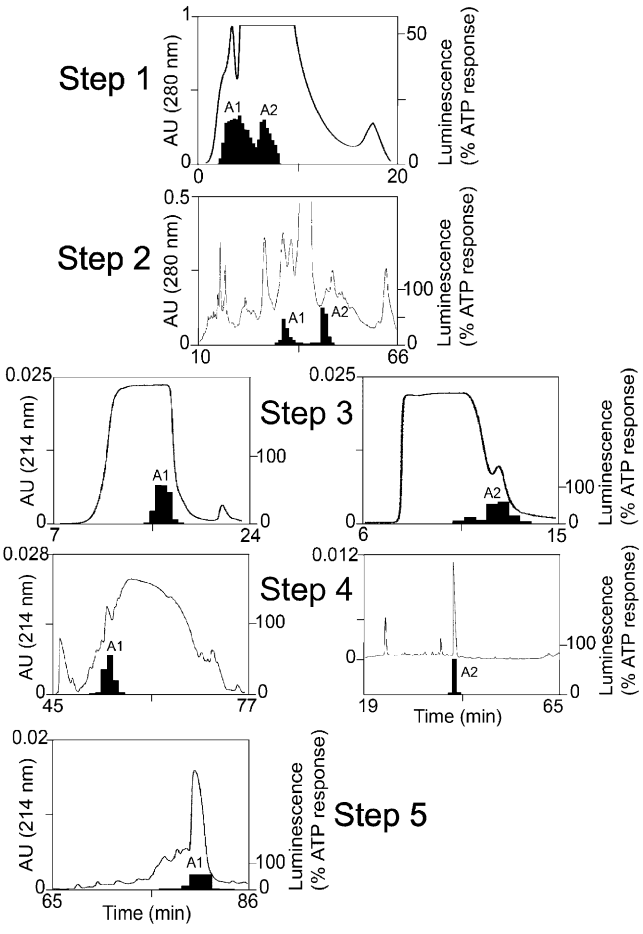

Figure 1. Purification from porcine spleen of the natural ligand of FPRL2. A porcine spleen homogenate was first fractionated by HPLC onto a Poros column (Step 1). The absorbance (AU) and biological activity on FPRL2-expressing CHO-K1 cells are shown. The luminescence measured in an aequorin-based assay (black bars) was normalized to the response obtained for 20 μM ATP. A1 (activity 1) and A2 (activity 2) represent the two active regions on the HPLC profile. They were processed together onto a C18 column (Step 2). Thereafter, A1 and A2 were purified separately onto an SEC (Step 3), a C4 column (Step 4), and for A1, a last C18 column (Step 5). The x axis is magnified to focus on the region of interest.

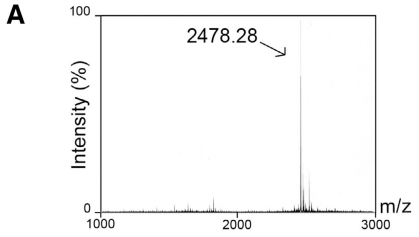

B

		Monoisotopic mass (dalton)	Sequence
Activity 1	Tryptic fragments	1978,03	NSLFGSVETWPWQVLSK
		1821,92	FATVEMTDKPVDEALR
Activity 2	Intact mass	2478,28	**Ac-MLGMIKNSLFGSVETWPWQVL**
	Tryptic fragment	1762,94	**NSLFGSVETWPWQVL**

C

```
Human   MLGMIKNSLFGSVETWPWQVLSKGDKEEVAYEERACEGGKFATVEVT
Mouse   MLGMIRNSLFGSVETWPWQVLSTGGKEDVSYEERACEGGKFATVEVT
Pig     MLGMIKNSLFGSVETWPWQVLSKGDKQDISYEERACEGGKFATVEMT

Human   DKPVDEALREAMPKVAKYAGGTNDKGIGMGMTVPISFAVFPNEDGS
Mouse   DKPVDEALREAMPKIMKYVGGTNDKGVGMGMTVPVSFAVFPNEDGS
Pig     DKPVDEALREAMPKVMKYVGGSNDKGIGMGMTVPISFAVFPSDGGS

Human   LQKKLKVWFRIPNQFQSDPPAPSDKSVKIEEREGITVYSMQFGGYAKE
Mouse   LQKKLKVWFRIPNQFQGSPPAPSDESVKIEEREGITVYSTQFGGYAKE
Pig     LQKKLKVWFRIPNEFQSNPPVPSDDSIKIEERESITVYSLQFGGYAKE

Human   ADYVAQATRLRAALEGT ATYRGDIYFCTGYDPPMKPYGRRNEIWLLKT
Mouse   ADYVAHATQLRTTLEGTPATYQGDVYYCAGYDPPMKPYGRRNEVWLVKA
Pig     ADYVARAAQLRTALEGI ATCRSDVYFCTGYDPPMKPYGRRNEVWLVKA
```

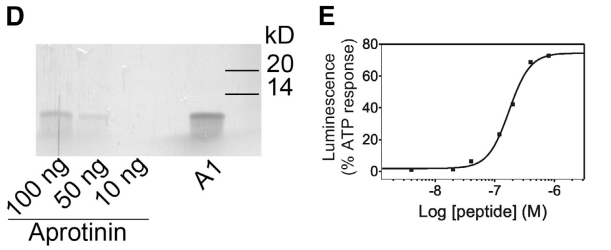

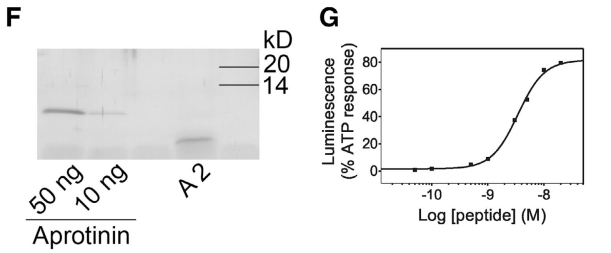

Figure 2. Identification of F2L as a high affinity natural ligand of FPRL2. (A) Mass spectrometry analysis of the undigested fraction A2 resulting from step 4 using a Maldi Q-TOF mass spectrometer. (B) Sequences corresponding to the major peaks of the mass spectra of trypsin-digested A1 (step 5) and A2 (step 4) fractions or undigested A2. All microsequenced peptides were found to derive from the porcine HBP. The F2L peptide (A2 fraction) is amino terminally acetylated. Ac, acetyl. (C) Amino acid sequence alignment of human, mouse, and porcine HBP. The sequence corresponding to the F2L peptide (represented in bold) is identical in human and porcine HBP. The region containing tryptic peptides recovered from fraction A1 is boxed (human HBP, NM 015987; murine HBP, NM 013546). (D) The A1 fraction (step 5) was migrated onto SDS-PAGE together with 10, 50, and 100 ng aprotinin as standards. The gel was silver stained, and it was estimated that the major band (6 kD) contained around 300 ng of peptide. (E) Biological activity of the A1 fraction on CHO-K1 cells expressing human FPRL2 using the aequorin-based assay. (F) The A2 fraction (step 4) was migrated onto SDS-PAGE together with 10 and 50 ng aprotinin as standards. The gel was silver stained and the amount of F2L (3 kD) was estimated to 40 ng. (G) Biological activity of F2L (A2, step 4) on CHO-K1 cells expressing human FPRL2 using the aequorin-based assay.

lowed us to test fractions from human lymphoid organ extracts, conditioned media of leukocyte populations, and inflammatory fluids. A biological activity, specific for FPRL2-expressing cell lines, was detected in fractions resulting from the reverse phase HPLC fractionation of extracts from human spleen (not depicted). For practical reasons, we tested fractions from porcine spleen prepared in a similar way and identified two regions of the profile containing specific activities for FPRL2 (activities A1 and A2; Fig. 1). Starting from 350 g of porcine spleen, these two activities were purified to homogeneity by five (A1) or four (A2) successive HPLC steps, the first two being common (Fig. 1). The sensitivity of both activities to proteinase K suggested a peptidic nature (not depicted). The molecular mass of the active compounds was estimated by size-exclusion chromatography to ~6 kD for activity A1 and 3 kD for activity A2. From the absorbance of the peaks and the biological activities associated with them, the compound present in peak A1 appeared more abundant but less active than that of peak A2. The two fractions were analyzed by SDS-PAGE and silver staining to quantify approximately the active peptides by comparison with known amounts of aprotinin and lysozyme (Fig. 2, D and F). A concentration action curve performed on the same fractions in the aequorin-based functional assay allowed us to estimate an EC_{50} of 2.32 ± 1.84 nM ($n = 2$) for A2 and 200 ± 54 nM ($n = 4$) for A1 (Fig. 2, G and E, respectively). Both peptides were analyzed by mass spectrometry, either without (A2) or after tryptic digestion (A1 and A2; Fig. 2, A and B). For A2, analysis of the undigested peptide allowed us to identify the entire microsequence as matching the first 21 amino acids of a human intracellular heme-binding protein (HBP; sequence data are available from GenBank/EMBL/DDBJ under accession no. NM 015987) with an amino-terminal acetylation (mol wt: 2,478.28 daltons; Fig. 2, A and B). For A1, six peptides, of which four were fragments of the two longest tryptic fragments shown in Fig. 2 B, were also consistent with HBP. The porcine HBP was cloned by PCR from liver cDNA using degenerate primers, which allowed us to confirm the identification, and the perfect conservation of the first 21 amino acids as compared with the human sequence. This sequence was later confirmed after the incorporation of porcine HBP expressed sequence tags in public databases (data available from GenBank/EMBL/DDBJ under accession no. AY662687). The two tryptic peptides from A1 covered 50 amino acids in the amino-terminal domain of the 190–amino acid-long sequence of porcine HBP (Fig. 2 C). We assume that the amino-terminal end of A1 is common to that of A2, although it could not be demonstrated. The carboxy-terminal end of A1 was not deter-

Table I. Pharmacology of FPRs

Receptor	Ligand	pEC_{50} (aequorin assay)	pEC_{50} (cAMP assay)	pIC_{50} (binding assay)
FPRL2	F2L	8.02 ± 0.13 (n = 9)	8.24 ± 0.06 (n = 4)	7.48 ± 0.003 (n = 3)
	WKYMVm	<6	NT	<6
	WKYMVM	<6	<6	NT
	SHAAG	<6	<6	<6
	FMLP	<6	<6	<6
FPRL1	F2L	6.26 ± 0.12 (n = 3)	6.65 ± 0.16 (n = 8)	<6
	WKYMVm	10.57 ± 0.10 (n = 3)	NT	7.66 ± 0.15 (n = 3)
	WKYMVM	10.04 ± 0.18 (n = 3)	10.27 ± 0.27 (n = 4)	NT
	SHAAG	9.27 ± 0.06 (n = 3)	9.23 ± 0.17 (n = 6)	NT
	FMLP	5.94 ± 0.03 (n = 3)	<6	NT
FPR	F2L	<6	<6	<6
	WKYMVm	9.18 ± 0.16 (n = 3)	NT	7.03 ± 0.16 (n = 3)
	WKYMVM	7.48 ± 0.08 (n = 3)	8.23 ± 0.13 (n = 4)	NT
	SHAAG	<6	<6	NT
	FMLP	9.39 ± 0.33 (n = 3)	10.15 ± 0.08 (n = 4)	NT

Binding and activation of CHO-K1 cells expressing FPRL2, FPRL1, or FPR by F2L, FMLP, WKYMVm, WKYMVM, and SHAAG were studied using a binding assay, an aequorin-based assay, and an assay measuring the inhibition of cAMP accumulation. The EC_{50} and IC_{50} parameters of the dose-response curves were determined by nonlinear regression using Graphpad Prism software. The results represent the mean pEC_{50} or pIC_{50} (-log values of EC_{50} or IC_{50}) ± SEM for at least three independent experiments (n).
NT, not tested.

mined precisely either, due to the large number of tryptic sites after Arg^{56} of HBP. The purification was performed three times with distinct protocols, and the same peptides were identified by mass spectrometry in each case.

Comparative pharmacology and intracellular signaling of FPRs

The pharmacology and signaling pathways activated by the three members of the human FMLP receptor family were investigated in CHO-K1 cells expressing the receptors with or without $G_{\alpha16}$ and apoaequorin (Fig. 3). The acetylated 21–amino acid peptide, named F2L (for FPRL2 ligand), was synthesized and tested in the aequorin-based assay on these three cell lines as well as on wild-type CHO-K1 cells and CHO-K1 cells expressing chemerinR and other GPCRs. The synthetic F2L peptide was shown to activate the FPRL2-expressing cells with a potency similar to that of the native peptide purified from the spleen and, with a much lower efficiency, FPRL1 and FPR (see below), but it was completely inactive on all other cell lines tested (not depicted). F2L was also tested in a cAMP accumulation assay on CHO-K1 cells expressing FPRL2 but not $G_{\alpha16}$. The synthetic peptide was found to inhibit the cAMP accumulation promoted by forskolin and was unable to stimulate cAMP production by itself. In the same cells, F2L also promoted intracellular calcium release at low nanomolar concentrations (not depicted) and induced at picomolar concentrations the phosphorylation of the extracellular signal–regulated kinase (ERK)1/2 mitogen-activated protein (MAP) kinases (Fig. 3 I). Kinetics study of MAP kinase activation showed a maximal phosphorylation at 15 min (Fig. 3 J). Calcium signaling was totally inhibited by pertussis toxin pretreatment, demonstrating the coupling of the FPRL2 receptor to the G_i family of heterotrimeric G proteins (Fig. 3 G).

The comparative pharmacology of the three FPRs was then studied in more detail, using F2L and four reference agonists of FPR and FPRL1 (FMLP, the hexapeptides WKYMVM and WKYMVm, and the CCL23-derived SHAAG peptide). Concentration action curves and the resulting functional parameters were established both in the aequorin-based assay and the cAMP accumulation assay after stimulation by 10 μM forskolin (Fig. 3, A and B, and Table I). Among the tested peptides, F2L was by far the most potent on FPRL2, with an EC_{50} of 10 nM in the aequorin assay and 5 nM in the cAMP assay. F2L also appeared as highly specific, as a weak activity was obtained on FPRL1 (EC_{50} of 567 and 234 nM in the aequorin and cAMP assays, respectively), whereas on FPR, only partial inhibition of cAMP accumulation was obtained for 1 μM F2L, and no activity was detected in the aequorin assay up to 5 μM. For the other peptides, the EC_{50} values obtained for FPR and FPRL1 (Table I) were essentially as described in the literature (3, 4, 13). However, significant differences with published data were observed when testing the two W hexapeptides on the FPRL2-expressing cells. Indeed, micromolar concentrations of these peptides were required to activate FPRL2 (while active at low nanomolar concentrations on FPR and FPRL1). As described, FMLP and SHAAG were inactive on FPRL2.

To further confirm that F2L is a specific high affinity ligand for FPRL2, we performed binding experiments. A modified F2L peptide bearing a carboxy-terminal tyrosine was found to display a potency similar to that of wild-type F2L in the aequorin assay (not depicted). This peptide was iodinated with ^{125}I and used as a tracer. Saturation binding assays, performed on FPRL2-expressing CHO-K1 cells, allowed us to determine a K_D of 11.7 ± 4.9 nM (n = 3) and a

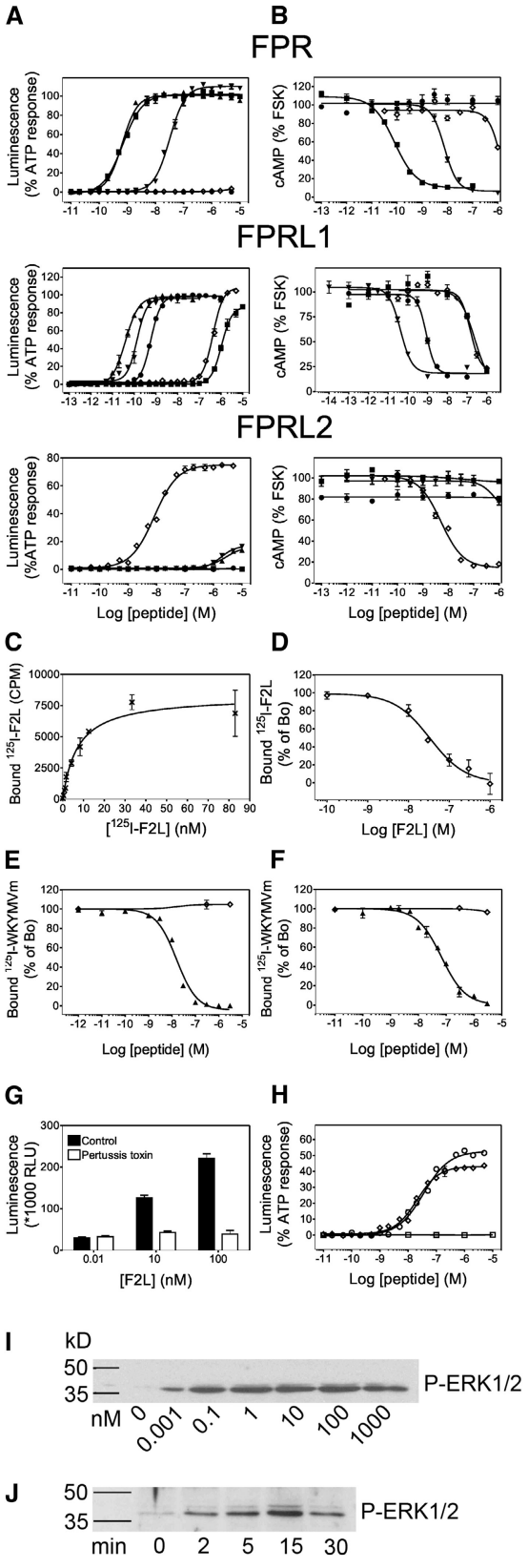

Figure 3. Pharmacology of the FPRs. (A) Concentration action curves of F2L (◇), FMLP (■), WKYMVm (▲), WKYMVM (▼), and SHAAG (●) peptides on CHO-K1 cells expressing FPR, FPRL1, or FPRL2 using the aequorin-based assay. Results are expressed as percentage of the response elicited by 20 μM ATP. (B) Concentration action curves of the same peptides on CHO-K1 cells expressing the three receptors using a cAMP accumulation assay. Results are expressed as percentage of the cAMP level obtained in the presence of 10 μM forskolin but in the absence of agonists. FSK, forskolin. (C) Saturation binding assay (specific binding) on FPRL2-expressing CHO-K1 cells using F2L bearing a carboxy-terminal [^{125}I]Tyr as tracer. (D) Competition binding assay on FPRL2-expressing CHO-K1 cells using F2L-[^{125}I]Tyr as tracer and F2L as competitor. (E and F) Competition binding assay on (E) FPRL1- and (F) FPR-expressing CHO-K1 cells using [^{125}I]-WKYMVm as tracer and WKYMVm (▲) or F2L (◇) as competitors. (G) Stimulation by F2L of FPRL2-expressing CHO-K1 cells cultured in the absence or presence of 100 ng/ml pertussis toxin using the aequorin-based assay. (H) Concentration action curves of acetylated (◇), nonacetylated (○), and [7–21]F2L (□) peptides on FPRL2-expressing CHO-K1 cells using the aequorin assay. (I) Immunodetection of phosphorylated ERK1/2 in FPRL2-expressing CHO-K1 cells after stimulation by F2L for 10 min. (J) Kinetics of ERK1/2 activation after stimulation by 100 nM F2L. Each experiment displayed in A–I was repeated at least three times.

B_{max} of roughly 30,000 receptors per cell (Fig. 3 C). Competition binding assays were performed with F2L, which displayed an IC_{50} of 33.4 ± 0.2 nM (Fig. 3 D and Table I). The hexapeptides WKYMVM and WKYMVm, SHAAG, and FMLP did not compete for FPRL2 binding up to concentrations of 3 μM (not depicted). Next, we confirmed the specificity of F2L for FPRL2 through binding experiments on FPR and FPRL1-expressing CHO-K1 cells using [^{125}I]-WKYMVm as a tracer. The IC_{50} values for WKYMVm were 22.5 ± 7.6 nM on FPRL1 (Fig. 3 E) and 98.4 ± 37.4 nM on FPR (Fig. 3 F), but no competition was observed for F2L up to concentrations of 3 μM.

By analogy with formyl peptides, we investigated the role of the amino-terminal acetylation of F2L. The nonacetylated peptide was synthesized and shown to display an EC_{50} for FPRL2 similar to that of acetylated F2L (21.1 ± 7.6 nM, $n = 3$; Fig. 3 H). We also tested a truncated F2L variant lacking the first six amino acids (F2L[7–21]) because mouse intracellular HBP was originally described by Edman sequencing as lacking this amino-terminal part (21). This truncated peptide was found to be totally inactive in aequorin (Fig. 3 H) and binding assay (not depicted).

Distribution of human FPRL2

We investigated the presence of FPRL2 transcripts in various leukocyte populations by RT-PCR (Fig. 4 A). As described previously (19), FPRL2 transcripts were the most abundant in monocytes and immature or mature monocyte-derived DCs. Maturation of DCs was induced by either LPS, LPS plus IFN-γ, or CD40L for 3–24 h, with no detectable variation of the level of expression of FPRL2 transcripts (Fig. 4 A and not depicted). They were either absent or present at very low levels in all other cell populations tested. Quantitative RT-PCR was performed on a number of tissues using DCs as reference. Transcripts were found at low levels in most tissues and at higher levels in the lymph nodes, small intestine, lung, and adipose tissue (Fig. 4 B).

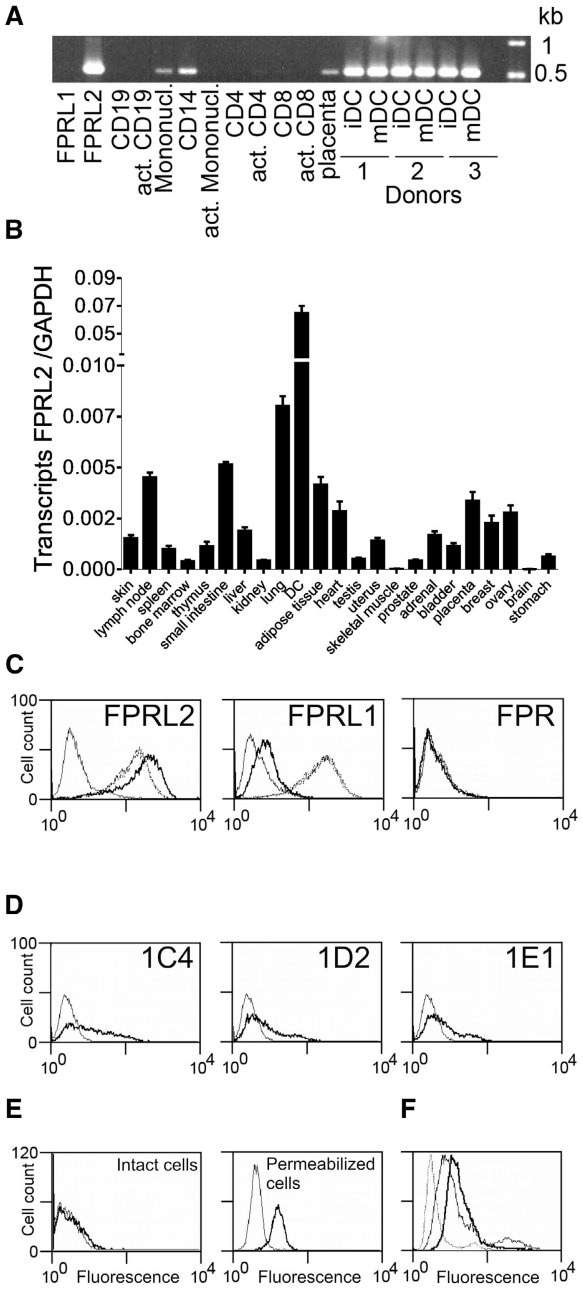

Figure 4. Expression profile of human FPRL2. (A) Transcripts encoding human FPRL2 were amplified by RT-PCR in a set of human leukocyte populations. act., activated; Mononucl., mononuclear cells; iDC, immature DCs; mDC, mature DCs. (B) Distribution of FPRL2 in a set of human tissues by using quantitative RT-PCR (Taqman). The data were normalized for the expression of GAPDH used as control. (C) Anti-FPRL2 monoclonal antibodies were characterized by FACS on CHO-K1 cells expressing FPR, FPRL1, and FPRL2. Bold solid line, 1C4; dotted line, 1D2; dashed line, 1E1; thin solid line, control labeling (IgG2a). The profiles of 1D2 and 1E1 are superimposed and cannot therefore be distinguished. (D) The expression of FPRL2 was analyzed by FACS on immature DCs using the three monoclonal antibodies. Bold solid line, anti-FPRL2 antibodies; thin solid line, control labeling (IgG2a). (E) Expression of FPRL2 on intact and permeabilized DCs using 1C4. Bold solid line, 1C4; thin solid line, control labeling (IgG2a). (F) Expression of FPRL2 on immature (bold solid line) and mature (thin solid line) DCs using 1D2. Dotted lines, control labeling (IgG2a).

Monoclonal antibodies were generated against human FPRL2 by genetic immunization and characterized by FACS on CHO-K1 cell lines expressing FPR, FPRL1, or FPRL2 (Fig. 4 C). One of the three monoclonals (1C4) was essentially specific for FPRL2, exhibiting poor recognition of FPRL1. The two other antibodies (1D2 and 1E1) recognized equally well both receptors. None, however, cross-reacted significantly with FPR. We investigated the ability of the antibodies to block F2L signaling on FPRL2-expressing CHO-K1 cells. However, their blocking properties appeared weak, as only partial inhibition of the signal was obtained with high concentrations (50 μg/ml) of 1C4 antibody (not depicted). These antibodies were used to confirm the presence of the receptor at the surface of DCs. The three monoclonals allowed us to detect FPRL2 on immature and mature monocyte-derived DCs, although at variable levels. FPRL2 expression could be detected in 16 out of 24 donors. The experiments on one representative donor are displayed in Fig. 4 D. We then compared intracytoplasmic and surface expression of FPRL2 on DCs by performing FACS analysis after permeabilization of the cells. We found significant intracellular expression of FPRL2 even for donors for which surface expression was very weak or undetectable (Fig. 4 E). Additionally, down-regulation of cell surface FPRL2 was observed when DCs were cultured in presence of 1 μM F2L for 48 h (not depicted). Together, these data suggest that the variation of expression among donors can be attributed to trafficking parameters such as internalization of the receptor after its stimulation by a ligand present in plasma. For four tested donors, maturation of DCs by LPS induced a slight decrease in surface expression of FPRL2 (Fig. 4 F). Finally, we evaluated the only variant of FPRL2 described to date (data available from GenBank/EMBL/DDBJ under accession no. AAA58482), which was characterized by an aspartic acid to histidine substitution at position 338. No difference in expression or functional response (cAMP inhibition) was detected after transient expression in HEK cells as compared with the FPRL2 form used initially (not depicted).

Biological activity of F2L in primary immune cells

The biological function of F2L was investigated on leukocyte populations. Given the role of FPR and FPRL1 in chemoattraction, and the distribution of FPRL2, we focused on the measurement of calcium mobilization and chemotaxis on monocytes and monocyte-derived DCs. F2L promoted intracellular Ca^{2+} flux in immature DCs (Fig. 5 A) as well as mature DCs (not depicted) in a dose-dependent manner. The amplitude of the response, although variable according to individuals, was comparable to that resulting from the stimulation by 10 nM FMLP (Fig. 5 B). The response was transient. According to the F2L concentration and the donor (not depicted), it went back to baseline after 1–3 min. Out of 12 donors tested, a strong response was obtained in 7 cases, a weak response in 2 cases, and no response for 3 donors. This is attributed to the variable expression level of FPRL2 as determined by FACS analysis. Calcium mobilization was also

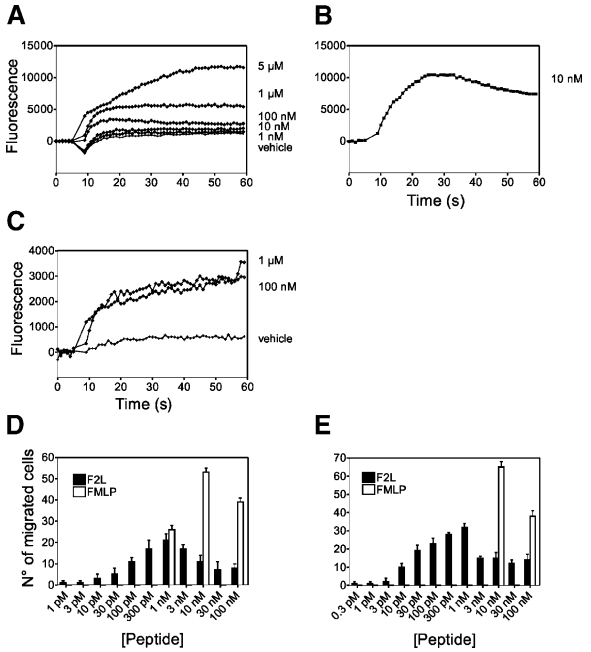

Figure 5. Biological activity of F2L on primary immune cells. (A and B) Recording of Ca^{2+} flux in monocyte-derived DCs in response to various concentrations of F2L (A) and 10 nM FMLP (B). (C) Recording of Ca^{2+} flux in monocytes in response to 100 nM and 1 μM F2L. (D and E) Chemotaxis of monocyte-derived human immature DCs (D) and PBMCs (E) in response to F2L. The displayed responses are representative of four donors out of five tested.

observed in purified monocytes in response to 100 nM F2L, although the amplitude of the signal was lower than with DCs (Fig. 5 C). Human F2L promoted ex vivo migration of immature DCs and monocytes (Fig. 5, D and E). Cell migration in response to F2L was mainly due to chemotaxis rather than chemokinesis as assessed in checkerboard experiments (not depicted). Maximal chemotactic responses were obtained for concentrations of 300 pM to 1 nM. The bell-shaped chemotactic response, with a maximum corresponding to concentrations below the EC_{50} derived from other functional assays, is typically observed for other chemotactic factors such as chemokines.

DISCUSSION

In the past few years, the functional characterization of orphan GPCRs has led to the identification of original pathophysiological pathways, promoting the use of these newly deorphanized receptors as candidate targets for drug development. The use of orphan receptors in various types of bioassays has indeed allowed the discovery of new biological mediators acting through GPCRs such as nociceptin/orphanin FQ, orexins, ghrelin, and chemerin, or to the identification of known molecules such as short fatty acids, succinate and α-ketoglutarate, and prostaglandins as the natural ligands of previously orphan GPCRs (22–28). Many of these receptors have since raised considerable interest for their role in human diseases and are now widely used in the drug discovery programs of the pharmaceutical industry.

The FPR family has been known for more than 10 yr. Two of its members, FPR and FPRL1, were found to respond to a number of endogenous or exogenous ligands and have been involved in numerous physiological and pathological processes, including antimicrobial defense, mounting of inflammatory responses, and development of amyloidogenic diseases. The third receptor of this family, FPRL2, had so far no high affinity natural agonist and was therefore still an orphan receptor. It displays an interesting expression profile, as it is selectively expressed in DCs and monocytes.

In this study, we have identified a natural ligand for FPRL2 by reverse pharmacology, using a bioassay based on the expression of the receptor in a recombinant cell line. Starting from the spleen, we have isolated and characterized a new peptide, F2L, as the first natural agonist displaying both high affinity and high selectivity for FPRL2. F2L is an acetylated 21–amino acid peptide derived from the amino-terminus of the intracellular HBP. It is highly conserved across mammalian species (Fig. 2 C). F2L binds and activates FPRL2 in the low nanomolar range, whereas the previously described ligands of the receptor (annexin I–derived Ac-1-25, bacterial Hp 2–20, and synthetic W peptides) are essentially FPRL1 agonists displaying weak activities on FPRL2. It should be noted that the synthetic hexapeptides WKYMVM and WKYMVm were initially described as high affinity agonists of FPRL2 on the basis of experiments conducted on purified leukocyte populations or FPRL2-expressing HL-60 cells (18, 19). Other data contradict these observations, describing activities of these peptides in the micromolar range on FPRL2 expressed in RINm5F (18) or HEK 293 cells (15). In our hands, these two peptides effectively required micromolar concentrations to elicit calcium influx in FPRL2-expressing CHO-K1 cells, whereas they were active at low nanomolar concentrations on FPR and FPRL1 expressed in the same system. It is likely that the early observations described above can be attributed to the endogenous expression of either FPR, FPRL1, or another unknown receptor in the systems used.

The amino-terminal methionine of F2L is acetylated, a modification that is found also in the amino-terminal peptide of annexin I, and is reminiscent of the formylated methionine of bacterial and mitochondrial peptides active on FPR. We have shown that the acetyl moiety is not essential for the activity of F2L in vitro, in contrast to the formyl group of FMLP. However, the acetyl-methionine might play an important role in stabilizing the peptide in vivo, protecting it from aminopeptidases and other proteases known to be activated in inflammatory situations.

Using blue sepharose chromatography, murine HBP was initially purified from the liver in a search for new cytosolic HBPs (21). Human HBP was later described as a monomeric tetrapyrolle-binding protein (29). HBP transcripts can be found in all tissues, but are particularly abundant in the kidney, liver, and spleen. In mouse erythroleukemia cells, HBP synthesis is stimulated by erythroid differentiation, and HBP antisense oligonucleotides partially block the increase

of heme content associated with this differentiation process (21). The putative function of HBP is to buffer heme and porphyrins synthesized in excess. As HBP is a cytosolic protein, its amino-terminal peptide fragments acting on FPRL2 could either be generated intracellularly by proteolytic processing and then released, or alternatively, the whole protein could be secreted and the cleavage could take place in the extracellular compartment. The longer, less active HBP-derived peptide isolated from the spleen could represent an intermediate step in the generation of the final, fully active agonist. HBP and/or its active fragments could be released either through a nonconventional mode of secretion or secondary to cell death. We did not observe biological activity on FPRL2-expressing cells in supernatants from CHO-K1 cells transfected with an expression vector containing the full-size human HBP cDNA (not depicted). This suggests that the processing leading to the active F2L peptide does not occur in CHO-K1 cells and probably requires a specific environment. An increasing number of proteins devoid of signal peptide were shown to be released from the cells by unknown mechanisms. IL-1β is generated from an intracellular precursor by proteolytic cleavage by the caspase ICE, and the unconventional mechanism by which it is released from the cells is not known (30). Two intracellular peptides, Sun A and B, were recently described as the ligands of the Drosophila receptor Methuselah (31). Annexin I, a ligand of FPR, FPRL1, and to a lower extent FPRL2, is also an intracellular protein of 346 amino acids, which is externalized by a still unclear mechanism when neutrophils adhere to the endothelium. The acetylated amino-terminal domain of the protein, which is exposed only in the presence of calcium ions (32), is cleaved by proteolysis, and both the full-size protein and the amino-terminal peptides bind the receptors (33, 34). Another recently identified ligand of FPRL1, humanin, is also an intracellular protein synthesized without signal peptide and shown to be released from cells in a nonconventional way. The humanin sequence was further shown to induce the secretion of other proteins when fused to them, thereby playing the role of an export signal (35).

F2L is a new member of the chemoattractant factor family. By binding on FPRL2, it triggers the classical intracellular cascades stimulated by chemoattractants through the G_i class of G proteins: stimulation of intracellular calcium release, inhibition of cAMP production, and activation of the MAP kinases ERK1/2. The peptide is able to chemoattract monocytes and immature DCs. It could therefore be involved in the response of these cells to infection, inflammation, or cell death. DCs are known to process and present antigens derived from infected, malignant, or allogeneic cells. Recent evidence indicates that these cells are attracted by dead or dying cells (36). The first self-molecules shown to represent danger signals were the heat shock proteins gp96 or hsp70. They are released from necrotic cells and are able to potently activate antigen-presenting cells (37). Intracellular nucleotides released under conditions of hypoxia, ischemia, inflammation, or mechanical stress, and crystalline uric acid deriving from dead cells, were also shown to stimulate DCs (38, 39). Apoptotic cells, in addition to engulfment signals, release chemotactic factors for phagocytes (40). Thus, it is conceivable that F2L, released from HBP by proteolysis after cell suffering or cell death, contributes to the chemoattraction of monocytes and DCs through FPRL2. Therefore, F2L and FPRL2 might be involved in the development of a number of inflammatory diseases associated with cell death. In this context, FPRL2 could represent an attractive target for therapeutic approaches. However, the characterization of the precise contribution of this system in specific human diseases will require additional investigations.

MATERIALS AND METHODS

Expression of human FPRL2, FPRL1, and FPR. The human coding sequences (data available from GenBank/EMBL/DDBJ accession nos AC005946, M84562, and M60626, respectively) were amplified by PCR from human genomic DNA, cloned into the pcDNA3 (Invitrogen) and pEFIN3 (Euroscreen) vectors, and sequenced. The pEFIN3 constructs were transfected using Fugene 6 into CHO-K1 cells expressing or not $G_{\alpha 16}$ and apoaequorin. G418-resistant clones were characterized for receptor expression by Northern blotting. A functional assay based on the luminescence of mitochondrial aequorin was performed as described previously (41). Results were expressed as relative light units or as the percentage of the response to 20 μM ATP.

Purification of bioactive peptides. 350 g of frozen porcine spleen was homogenized in four volumes of ice-cold 20% CH_3CN in water. The homogenate was centrifuged at 10,000 *g* for 30 min at 4°C and snap-frozen in liquid nitrogen. Aliquots of 200 ml of supernatant were diluted fourfold in 0.1% TFA and loaded on a Poros R2 bead 4.6 × 150–mm column (Applied Biosystems) at 5 ml/min. A 5–70% CH_3CN gradient (6%/min) in 0.1% TFA was applied, and 1.25 ml fractions were collected and tested for functional activity on FPRL2-expressing CHO-K1 cells in an aequorin assay. Two regions of activity (A1 and A2) were detected on the HPLC profile. The corresponding fractions were pooled, diluted fourfold in 0.1% TFA, and loaded at 1 ml/min on a C18 4.6 × 250–mm column (Vydac), which was submitted to a 30–50% CH_3CN gradient in 0.1% TFA. Two regions of activity were detected and subsequently treated separately. The 1-ml fractions corresponding to the first (A1, lower CH_3CN concentration) and the second (A2, higher CH_3CN concentration) regions from two runs were vacuum concentrated to 50 μl. A1 and A2 were diluted threefold in 30% CH_3CN/0.05% TFA and 30% CH_3CN/0.1% TFA, respectively, and loaded on size-exclusion columns (SECs; A1: TSK-gel Alpha-4000 [7.8 × 300 mm; Tosoh Biosep]; A2: Superdex peptide PE [7.5 × 300 mm; Amersham Biosciences) submitted to a 0.5 ml/min flow rate of dilution medium. The active 0.25-ml fractions from one SEC were diluted fourfold in 0.1% TFA and loaded at 0.2 ml/min on a C4 2.1 × 250–mm column (Vydac), which was submitted to a 25–45% (A1) or 30–50% (A2) CH_3CN gradient at 0.3%/min in 0.1% TFA. The fractions were collected manually according to the absorbance profile. For A1, the active fractions from one run were pooled, diluted fivefold in 0.1% TFA, and loaded at 0.05 ml/min on a C18 1 × 250–mm column (Vydac), which was submitted to a 23–50% CH_3CN gradient at 0.45%/min in 0.1% TFA. The fractions were collected manually. For A2, the purity of the final active fraction was checked by loading an aliquot on a C18 1 × 250–mm column. The purification was repeated three times with different protocols (i.e., the SEC step was replaced by a reverse phase step on a C18 2.1 × 250–mm column submitted to a CH_3CN gradient in 0.1% H_3PO_4 as ion-pairing agent). The protein concentration in active fractions was determined after SDS/PAGE by comparison with aprotinin and lysozyme standards after silver staining.

Mass spectrometry analysis. The active fractions were vacuum dried, resuspended in 20 mM ammonium bicarbonate, heated to 100°C for 5 min,

digested by 50 ng trypsin overnight or left intact, and purified by solid phase extraction (C18 ZipTip; Millipore). The peptides were eluted in 1.5 μl of 70% CH_3CN/0.1% TFA onto a metallic MALDI target, dried, and then mixed with 1.5 μl of matrix mix (2 mg/ml 2,5-dihydroxybenzoic acid and 10 mg/ml α-cyano-4-hydroxycinnamic acid, 2 mM fucose, 5 mM ammonium acetate). Mass spectrometry analysis was performed on a Q-TOF Ultima Global mass spectrometer equipped with a MALDI source (Micromass) and calibrated using the monoisotopic masses of tryptic and chymotryptic peptides from bovine serum albumin. Ionization was achieved using a nitrogen laser (337-nm beam, 10 Hz), and acquisitions were performed in a V mode reflectron position. Microsequencing was performed by argon-induced fragmentation after selection of the parent ion.

Synthetic peptides. Acetylated or nonacetylated MLGMIKNSLFGSVETWPWQVL (HBP[1–21], renamed F2L), NSLFGSVETWPWQVL (F2L[7–21]), WKYMVM, and MLWRRKIGPQMTLSHAAG (SHAAG peptide derived from CCL23 amino-terminus) were synthesized locally by using the solid phase Fmoc strategy (42) or were custom made by Eurogentec. WKYMVM and WKYMVm were purchased from Phoenix Pharmaceuticals and FMLP was purchased from Neosystem. Monoisotopic masses and sequences of all peptides were verified by mass spectrometry. F2L and WKYMVM from different origins displayed the same properties. At high concentrations, HBP-derived peptides were dissolved in DMSO and heated at 50°C for 10 min due to their high hydrophobicity. Intermediate dilutions were made in 50% CH_3CN and were further diluted 40-fold in assay buffer to reach working concentration.

Quantitative RT-PCR. FPRL2 transcripts were detected by RT-PCR in cDNA from human blood cell populations obtained commercially (CLONTECH Laboratories, Inc.) or prepared locally as described previously (43). Primers for FPRL2 were 5′-CTGGCCACACCGTTCTGT-3′ as forward and 5′-GGCCATGGTAATGAACACGTT-3′ as reverse. Amplification of GAPDH transcripts was performed as a control of the quality of cDNA (not depicted). FPRL2 transcripts were detected by quantitative RT-PCR (TaqMan) in total or polyA$^+$ RNA samples from human tissues obtained commercially (CLONTECH Laboratories, Inc. and Ambion) or prepared locally (DCs). Primers for FPRL2 were 5′-TTACCATGGCCAAGGTCTTTCT-3′ as forward, 5′-GCAGACTGTGATGATGGACATAGG-3′ as reverse, and 5′FAM-TCCTCCACTTCATTATTGGCTTCAGCGT-3′DABSYL as probe, and for the reference housekeeping gene (GAPDH) were 5′-GAAGGTGAAGGTCGGAGTC-3′ as forward, 5′-GAAGATGGTGATGGGATTTC-3′ as reverse, and 5′FAM-CAAGCTTCCCGTTCTCAGCC-3′DABSYL as probe. Primers were used at 900 nM and probes were used at 200 nM. Standard curves were run systematically for the two genes, and the transcript copy number of FPRL2 was normalized to the GAPDH transcript copy number for each sample.

Monoclonal antibodies and flow cytometry. BALB/c mice were injected with 100 μg pcDNA3-FPRL2 as described previously (44). Sera were tested by FACS on the CHO-K1-FPRL2 cell line, and immune mice were used to generate monoclonal antibodies by standard hybridoma technology using the NSO myeloma cell line. The Ig class of selected hybridomas was determined with a mouse monoclonal antibody isotyping kit (IsoStrip; Boehringer). Flow cytometry was performed using anti-FPRL2 antibodies or control IgG2a at 1 μg/ml (for CHO-K1 cells) or 5 μg/ml (for primary cells) in PBS containing 0.1% BSA, 0.1% sodium azide, and FITC-conjugated γ chain–specific goat anti–mouse IgG (Sigma-Aldrich) as secondary antibody. Fluorescence of 10,000 cells was assayed using a FACScan flow cytofluorimeter (Becton Dickinson). Intracytoplasmic staining was performed using the Cytoperm/Cytowash kit (Becton Dickinson) according to the manufacturer's instructions.

Intracellular cascade assays. The cAMP concentrations were determined using a homogeneous time-resolved fluorescence kit (Cis Bio International). In brief, cells were detached, resuspended in Krebs-Ringer hepes (KRH) buffer containing 1 mM 3-isobutyl-1-methylxanthine, and submitted to 10 μM forskolin alone or together with increasing concentrations of agonists for 30 min at room temperature. The reaction was stopped by the successive addition of cAMP-XL665 and anti-cAMP cryptate diluted in lysis buffer. The plates were incubated for 60 min at room temperature and read on a Rubystar fluorimeter (Labtech). Results were calculated from the 665:620 nm ratio and expressed in delta F (%). A calibration curve was obtained by plotting delta F% versus cAMP concentrations. ERK1/2 activation was assayed by Western blotting using an anti–phospho-p42/44 monoclonal antibody (E10; Cell Signaling Technology) as described previously (45). The aequorin-based assay was performed with or without overnight pretreatment with 100 ng/ml pertussis toxin. It was shown that such pertussis toxin pretreatment did not inhibit the functional response to ATP in these cells. For the analysis of FPRL2 polymorphism, HEK cells were transfected with a pcDNA3 vector containing the wild-type or Asp338His FPRL2 cDNA by the calcium phosphate method. Cells were recovered 48 h later and used for FACS or cAMP accumulation experiments.

Binding assays. F2L with an additional carboxy-terminal tyrosine was synthesized and found to display an EC_{50} similar to that of wild-type F2L in the aequorin assay. 5 μg of peptide was labeled with 2 mCi of ^{125}I using the Iodogen method (42). After separation of unbound ^{125}I, the resulting specific activity of the peptide was estimated to 900 Ci/mmole. [^{125}I]-WKYMVm (2,200 Ci/mmole) was purchased from PerkinElmer. FPRL2, FPRL1, and FPR-expressing CHO-K1 cells were plated in 24-well plates (200,000 cells per well for FPRL2 and 100,000 cells per well for the two other receptors). The next day, the cells were washed twice with a KRH buffer without NaCl containing 280 mM saccharose and, for FPRL1 and FPR, 0.1% NaN_3. For saturation binding assays, cells were incubated with various amounts of F2L-[^{125}I]Tyr and nonspecific binding was determined by using 1 μM F2L as competitor. For competition binding assays, cells were incubated with 100,000 cpm of F2L-[^{125}I]Tyr or 10,000 cpm of [^{125}I]-WKYMVm and various amounts of F2L or other peptides as competitors in KRH buffer supplemented with 5% BSA for 90 min at room temperature. Cells were washed twice with ice cold buffer, and total radioactivity was recovered with 1 M NaOH and counted in a gamma counter for 2 min.

Chemotaxis and Ca^{2+} mobilization assays on primary cells. Monocyte-derived DCs were generated either from the adherent fraction of PBMCs cultured with 800 U/ml GM-CSF and 500 U/ml Il-4, or from Percoll-purified monocytes cultured with 50 ng/ml GM-CSF and 20 ng/ml IL-13 for 5–7 d. For Ca^{2+} mobilization assay, monocytes were obtained by negative selection with the Monocyte Isolation Kit II (Miltenyi Biotec). Cell migration in response to F2L and FMLP and MIP-1α (CCL3) used as controls was evaluated by using a 48-well microchemotaxis chamber technique as described previously (2). For Ca^{2+} mobilization assays, monocyte-derived DCs or monocytes (5×10^5 cells/ml in HBSS without phenol red but containing 0.1% BSA and 1 mM Probenecid; Sigma-Aldrich) were loaded with 4 μM Fluo 4 (Molecular Probes) for 1 h at 20°C in the dark. The loaded cells were washed twice, resuspended at $1–2 \times 10^6$ cells/ml, and 50 μl of cell suspension was distributed per well in a 96-well plate (Viewplate; Packard Instrument Co.). Reading was performed in a Fluostar fluorimeter (Labtech) at 25°C. 50 μl of ligand-containing medium was injected, and the fluorescence at 520 nm was recorded every second for 1–3 min. Each condition was performed in triplicate, the mean fluorescence for each time point was calculated, and the curves were normalized by subtracting the mean value of the five measurements preceding the injection.

We thank Dominique Revets, Naïma Alaouï, and Nadia Tazir for their expert technical assistance, and Drs. Valérie Panneels, Frédéric Sallman, Stanislas Goriely, and Sophie Noël for expert advice. We are grateful to Dr. Luc De Pauw for providing human clinical samples.

This work was supported by the Belgian program on Interuniversity Poles of Attraction initiated by the Belgian State, Prime Minister's Office, Science Policy Programming, the LifeSciHealth program of the European Community (grant LSHB-CT-2003-503337), the Fonds de la Recherche Scientifique Médicale of Belgium,

Fortis, and the Fondation Médicale Reine Elisabeth to M. Parmentier. This work was partially supported by the Associazone Italiana per la Ricerca sul Cancro (AIRC) and by the Ministero dell'Istruzione, Università e Ricerca (MIUR). The scientific responsibility is assumed by the authors. I. Migeotte is Aspirant and D. Communi is Research Associate of the Belgian Fonds National de la Recherche Scientifique. V. Wittamer was recipient of grants from the FIRST-Industrie program of the Walloon Region and Télévie. J.-D. Franssen, C. Loison, and M. Detheux are employees of Euroscreen, which has the exploitation right regarding the work described.

The authors have no other conflicting financial interests.

Submitted: 25 June 2004
Accepted: 22 November 2004

Note added in proof. After acceptance of this manuscript, Harada et al. reported humanin as a high affinity ligand for FPRL2 (Harada, M., Y. Habata, M. Hosoya, K. Nishi, R. Fujii, M. Kobayashi, and S. Hinuma. 2004. *Biochem. Biophys. Res. Commun.* 324:255–261.)

REFERENCES

1. Lipscomb, M.F., and B.J. Masten. 2002. Dendritic cells: immune regulators in health and disease. *Physiol. Rev.* 82:97–130.
2. Wittamer, V., J.D. Franssen, M. Vulcano, J.F. Mirjolet, E. Le Poul, I. Migeotte, S. Brezillon, R. Tyldesley, C. Blanpain, M. Detheux, et al. 2003. Specific recruitment of antigen-presenting cells by chemerin, a novel processed ligand from human inflammatory fluids. *J. Exp. Med.* 198:977–985.
3. Le, Y., J.J. Oppenheim, and J.M. Wang. 2001. Pleiotropic roles of formyl peptide receptors. *Cytokine Growth Factor Rev.* 12:91–105.
4. Le, Y., P.M. Murphy, and J.M. Wang. 2002. Formyl-peptide receptors revisited. *Trends Immunol.* 23:541–548.
5. Boulay, F., M. Tardif, L. Brouchon, and P. Vignais. 1990. Synthesis and use of a novel N-formyl peptide derivative to isolate a human N-formyl peptide receptor cDNA. *Biochem. Biophys. Res. Commun.* 168:1103–1109.
6. Bao, L., N.P. Gerard, R.L. Eddy Jr., T.B. Shows, and C. Gerard. 1992. Mapping of genes for the human C5a receptor (C5AR), human FMLP receptor (FPR), and two FMLP receptor homologue orphan receptors (FPRH1, FPRH2) to chromosome 19. *Genomics.* 13:437–440.
7. Murphy, P.M., T. Ozcelik, R.T. Kenney, H.L. Tiffany, D. McDermott, and U. Francke. 1992. A structural homologue of the N-formyl peptide receptor. Characterization and chromosome mapping of a peptide chemoattractant receptor family. *J. Biol. Chem.* 267:7637–7643.
8. Gao, J.L., H. Chen, J.D. Filie, C.A. Kozak, and P.M. Murphy. 1998. Differential expansion of the N-formylpeptide receptor gene cluster in human and mouse. *Genomics.* 51:270–276.
9. Wang, Z.G., and R.D. Ye. 2002. Characterization of two new members of the formyl peptide receptor gene family from 129S6 mice. *Gene.* 299:57–63.
10. Walther, A., K. Riehemann, and V. Gerke. 2000. A novel ligand of the formyl peptide receptor: annexin I regulates neutrophil extravasation by interacting with the FPR. *Mol. Cell.* 5:831–840.
11. Le, Y.Y., W.H. Gong, B.Q. Li, N.M. Dunlop, W.P. Shen, S.B. Su, R.D. Ye, and J.M. Wang. 1999. Utilization of two seven-transmembrane, G protein-coupled receptors, formyl peptide receptor-like 1 and formyl peptide receptor, by the synthetic hexapeptide WKYMVm for human phagocyte activation. *J. Immunol.* 163:6777–6784.
12. Sun, R., P. Iribarren, N. Zhang, Y. Zhou, W. Gong, E.H. Cho, S. Lockett, O. Chertov, F. Bednar, T.J. Rogers, et al. 2004. Identification of neutrophil granule protein cathepsin G as a novel chemotactic agonist for the G protein-coupled formyl peptide receptor. *J. Immunol.* 173:428–436.
13. Elagoz, A., D. Henderson, P.S. Babu, S. Salter, C. Grahames, L. Bowers, M.O. Roy, P. Laplante, E. Grazzini, S. Ahmad, and P.M. Lembo. 2004. A truncated form of CKbeta8-1 is a potent agonist for human formyl peptide-receptor-like 1 receptor. *Br. J. Pharmacol.* 141:37–46.
14. Ying, G., P. Iribarren, Y. Zhou, W. Gong, N. Zhang, Z.X. Yu, Y. Le, Y. Cui, and J.M. Wang. 2004. Humanin, a newly identified neuroprotective factor, uses the G protein-coupled formylpeptide receptor-like-1 as a functional receptor. *J. Immunol.* 172:7078–7085.
15. Ernst, S., C. Lange, A. Wilbers, V. Goebeler, V. Gerke, and U. Rescher. 2004. An annexin 1 N-terminal peptide activates leukocytes by triggering different members of the formyl peptide receptor family. *J. Immunol.* 172:7669–7676.
16. Betten, A., J. Bylund, T. Cristophe, F. Boulay, A. Romero, K. Hellstrand, and C. Dahlgren. 2001. A proinflammatory peptide from *Helicobacter pylori* activates monocytes to induce lymphocyte dysfunction and apoptosis. *J. Clin. Invest.* 108:1221–1228.
17. De Paulis, A., N. Prevete, I. Fiorentino, A.F. Walls, M. Curto, A. Petraroli, V. Castaldo, P. Ceppa, R. Fiocca, and G. Marone. 2004. Basophils infiltrate human gastric mucosa at sites of *Helicobacter pylori* infection, and exhibit chemotaxis in response to *H. pylori*-derived Peptide Hp(2-20). *J. Immunol.* 172:7734–7743.
18. Christophe, T., A. Karlsson, C. Dugave, M.J. Rabiet, F. Boulay, and C. Dahlgren. 2001. The synthetic peptide Trp-Lys-Tyr-Met-Val-Met-NH2 specifically activates neutrophils through FPRL1/lipoxin A4 receptors and is an agonist for the orphan monocyte-expressed chemoattractant receptor FPRL2. *J. Biol. Chem.* 276:21585–21593.
19. Yang, D., Q. Chen, B. Gertz, R. He, M. Phulsuksombati, R.D. Ye, and J.J. Oppenheim. 2002. Human dendritic cells express functional formyl peptide receptor-like-2 (FPRL2) throughout maturation. *J. Leukoc. Biol.* 72:598–607.
20. Yang, D., Q. Chen, Y. Le, J.M. Wang, and J.J. Oppenheim. 2001. Differential regulation of formyl peptide receptor-like 1 expression during the differentiation of monocytes to dendritic cells and macrophages. *J. Immunol.* 166:4092–4098.
21. Taketani, S., Y. Adachi, H. Kohno, S. Ikehara, R. Tokunaga, and T. Ishii. 1998. Molecular characterization of a newly identified heme-binding protein induced during differentiation of murine erythroleukemia cells. *J. Biol. Chem.* 273:31388–31394.
22. He, W., F.J. Miao, D.C. Lin, R.T. Schwandner, Z. Wang, J. Gao, J.L. Chen, H. Tian, and L. Ling. 2004. Citric acid cycle intermediates as ligands for orphan G protein-coupled receptors. *Nature.* 429:188–193.
23. Hirai, H., K. Tanaka, O. Yoshie, K. Ogawa, K. Kenmotsu, Y. Takamori, M. Ichimasa, K. Sugamura, M. Nakamura, S. Takano, and K. Nagata. 2001. Prostaglandin D2 selectively induces chemotaxis in T helper type 2 cells, eosinophils, and basophils via seven-transmembrane receptor CRTH2. *J. Exp. Med.* 193:255–261.
24. Im, D.S. 2002. Orphan G protein-coupled receptors and beyond. *Jpn. J. Pharmacol.* 90:101–106.
25. Itoh, Y., Y. Kawamata, M. Harada, M. Kobayashi, R. Fujii, S. Fukusumi, K. Ogi, M. Hosoya, Y. Tanaka, H. Uejima, et al. 2003. Free fatty acids regulate insulin secretion from pancreatic beta cells through GPR40. *Nature.* 422:173–176.
26. Joost, P., and A. Methner. 2002. Phylogenetic analysis of 277 human G protein-coupled receptors as a tool for the prediction of orphan receptor ligands. *Genome Biol.* 3:RESEARCH0063.1–0063.16.
27. Lee, D.K., S.R. George, and B.F. O'Dowd. 2003. Continued discovery of ligands for G protein-coupled receptors. *Life Sci.* 74:293–297.
28. Meunier, J.C., C. Mollereau, L. Toll, C. Suaudeau, C. Moisand, P. Alvinerie, J.L. Butour, J.C. Guillemot, P. Ferrara, B. Monsarrat, et al. 1995. Isolation and structure of the endogenous agonist of opioid receptor-like ORL1 receptor. *Nature.* 377:532–535.
29. Jacob, B.B., T.A. Dailey, X. Lianchun, and H.A. Dailey. 2002. Characterization of a human and mouse tetrapyrrole-binding protein. *Arch. Biochem. Biophys.* 407:196–201.
30. Nickel, W. 2003. The mystery of nonclassical protein secretion. A current view on cargo proteins and potential export routes. *Eur. J. Biochem.* 270:2109–2119.
31. Cvejic, S., Z. Zhu, S.J. Felice, Y. Berman, and X.Y. Huang. 2004. The endogenous ligand Stunted of the GPCR Methuselah extends lifespan in *Drosophila*. *Nat. Cell Biol.* 6:540–546.
32. Rosengarth, A., and H. Luecke. 2003. A calcium-driven conformational switch of the N-terminal and core domains of annexin A1. *J. Mol. Biol.* 326:1317–1325.
33. Perretti, M., N. Chiang, M. La, I.M. Fierro, S. Marullo, S.J. Getting, E. Solito, and C.N. Serhan. 2002. Endogenous lipid- and peptide-derived

anti-inflammatory pathways generated with glucocorticoid and aspirin treatment activate the lipoxin A4 receptor. *Nat. Med.* 8:1296–1302.
34. Gavins, F.N., S. Yona, A.M. Kamal, R.J. Flower, and M. Perretti. 2003. Leukocyte antiadhesive actions of annexin 1. *Blood.* 101:4140–4147.
35. Yamagishi, Y., Y. Hashimoto, T. Niikura, and I. Nishimoto. 2003. Identification of essential amino acids in Humanin, a neuroprotective factor against Alzheimer's disease-relevant insults. *Peptides.* 24:585–595.
36. Pulendran, B. 2004. Immune activation: death, danger and dendritic cells. *Curr. Biol.* 14:R30–R32.
37. Binder, R.J., K.M. Anderson, S. Basu, and P.K. Srivastava. 2000. Cutting edge: heat shock protein gp96 induces maturation and migration of CD11c+ cells in vivo. *J. Immunol.* 165:6029–6035.
38. la Sala, A., D. Ferrari, F. Di Virgilio, M. Idzko, J. Norgauer, and G. Girolomoni. 2003. Alerting and tuning the immune response by extracellular nucleotides. *J. Leukoc. Biol.* 73:339–343.
39. Shi, Y., J.E. Evans, and K.L. Rock. 2003. Molecular identification of a danger signal that alerts the immune system to dying cells. *Nature.* 425: 516–521.
40. Lauber, K., E. Bohn, S.M. Krober, Y.J. Xiao, S.G. Blumenthal, R.K. Lindemann, P. Marini, C. Wiedig, A. Zobywalski, S. Baksh, et al. 2003. Apoptotic cells induce migration of phagocytes via caspase 3-mediated release of a lipid attraction signal. *Cell.* 113:717–730.
41. Stables, J., A. Green, F. Marshall, N. Fraser, E. Knight, M. Sautel, G. Milligan, M. Lee, and S. Rees. 1997. A bioluminescent assay for agonist activity at potentially any G protein-coupled receptor. *Anal. Biochem.* 252:115–126.
42. Gourlet, P., J. Rathe, P. De Neef, J. Cnudde, M.C. Vandermeers-Piret, M. Waelbroeck, and P. Robberecht. 1998. Interaction of lipophilic VIP derivatives with recombinant VIP1/PACAP and VIP2/PACAP receptors. *Eur. J. Pharmacol.* 354:105–111.
43. Migeotte, I., J.D. Franssen, S. Goriely, F. Willems, and M. Parmentier. 2002. Distribution and regulation of expression of the putative human chemokine receptor HCR in leukocyte populations. *Eur. J. Immunol.* 32:494–501.
44. Costagliola, S., P. Rodien, M.C. Many, M. Ludgate, and G. Vassart. 1998. Genetic immunization against the human thyrotropin receptor causes thyroiditis and allows production of monoclonal antibodies recognizing the native receptor. *J. Immunol.* 160:1458–1465.
45. Kotani, M., M. Detheux, A. Vandenbogaerde, D. Communi, J.M. Vanderwinden, E. Le Poul, S. Brezillon, R. Tyldesley, N. Suarez-Huerta, F. Vandeput, et al. 2001. The metastasis suppressor gene KiSS-1 encodes kisspeptins, the natural ligands of the orphan G protein-coupled receptor GPR54. *J. Biol. Chem.* 276:34631–34636.